

# UC Berkeley

## UC Berkeley Previously Published Works

### Title

Chilled ceiling and displacement ventilation system: Laboratory study with high cooling load

### Permalink

<https://escholarship.org/uc/item/7mf679pf>

### Journal

Science and Technology for the Built Environment, 21(7)

### ISSN

2374-4731

### Authors

Schiavon, Stefano  
Bauman, Fred S  
Tully, Brad  
[et al.](#)

### Publication Date

2015-10-03

### DOI

10.1080/23744731.2015.1034061

Peer reviewed



## Chilled ceiling and displacement ventilation system: Laboratory study with high cooling load

Stefano Schiavon, Fred S. Bauman, Brad Tully & Julian Rimmer

To cite this article: Stefano Schiavon, Fred S. Bauman, Brad Tully & Julian Rimmer (2015): Chilled ceiling and displacement ventilation system: Laboratory study with high cooling load, Science and Technology for the Built Environment, DOI: [10.1080/23744731.2015.1034061](https://doi.org/10.1080/23744731.2015.1034061)

To link to this article: <http://dx.doi.org/10.1080/23744731.2015.1034061>



Accepted online: 18 Apr 2015. Published online: 18 Apr 2015.



Submit your article to this journal [↗](#)



Article views: 47



View related articles [↗](#)



View Crossmark data [↗](#)



Citing articles: 1 View citing articles [↗](#)

# Chilled ceiling and displacement ventilation system: Laboratory study with high cooling load

STEFANO SCHIAVON<sup>1,\*</sup>, FRED S. BAUMAN<sup>1</sup>, BRAD TULLY<sup>2</sup>, and JULIAN RIMMER<sup>3</sup>

<sup>1</sup>Center for the Built Environment (CBE), University of California, Berkeley, 390 Wurster Hall #1839, Berkeley, CA 94720–1839, USA

<sup>2</sup>Price Industries Incorporated, Winnipeg, Manitoba, Canada

<sup>3</sup>Price Industries Incorporated, Suwanee, GA, USA

Radiant chilled ceilings with displacement ventilation represent a promising system that combines the energy efficiency of both subsystems with the opportunity for improved ventilation performance. Laboratory experiments were conducted for an interior zone office with a very high cooling load ( $91.0 \text{ W/m}^2$ ) and with two different heat source heights to investigate their influence on thermal stratification and air change effectiveness. The results showed that displacement ventilation with a chilled ceiling is able to provide a stable thermal stratification and improved ventilation effectiveness compared to mixing ventilation for a wide range of configurations. Stratification and air change effectiveness decreases when a larger portion of the cooling load is removed by the chilled ceiling. For every degree decrement of the surface temperature of the radiant ceiling, the stratification decreases by 0.13 K and the air change effectiveness by 0.13. Moving the computer processing units (representing 51% of the total room heat gain) from the floor level to 1.5 m height markedly increased the room median stratification and the median air change effectiveness (from 1.15 to 2.90). Therefore, increasing the height of heat sources has the potential to reduce energy use and improve indoor air quality.

## Introduction

Displacement ventilation (DV) is a room air distribution strategy that can improve indoor air quality compared to overhead mixing systems. In a DV system, air is supplied at very low velocity through supply devices located near floor level (most commonly side-wall diffusers) and is returned near ceiling level. A displacement flow pattern can also be obtained with horizontal discharge (low throw) floor diffusers in under-floor air distribution (UFAD) systems. ASHRAE (Chen and Glicksman 2003) and REHVA (Skistad et al. 2002) methods are the most commonly used references for the design and operation of DV systems. Hydronic-based radiant systems have been associated with significant energy savings (Feustel and Stetiu 1995; Stetiu 1999; Tian and Love 2005; Leach et al. 2010; Thornton et al. 2009; Sastry and Rumsey 2014), even if sometimes problems could arise (e.g., simultaneous heating and cooling [Tian and Love 2009] and incorrect cooling load

estimation [Feng et al. 2013, 2014]); therefore, there is strong interest in combining hydronic systems with the indoor air quality benefits of DV.

A review of the literature about DV and the radiant chilled ceiling (CC) until 2010 was reported in Schiavon et al. (2012). A short summary of the literature review and updates based on recently published works is reported hereafter. The combination of a chilled floor and DV was described in Causone et al. (2010), who concluded that the combination of DV with floor cooling, under a typical European office room layout, may cause the air temperature difference between the head and ankles to exceed the comfort range specified by ASHRAE Standard 55–2013 (ASHRAE 2013a). They also noticed that by increasing the airflow rate and thus raising the floor temperature, the vertical air temperature differences decreased. They also showed that the draft risk did not increase significantly. From the indoor air quality point of view, they showed that the presence of the chilled radiant floor does not affect the contaminant-removal effectiveness of the DV system.

The combination of CC and DV is more attractive for U.S. commercial building markets. There are two types of CC designs: (1) radiant ceiling panels and (2) thermally activated building systems (TABS). Radiant ceiling panels have several advantages: fast response time, ease of design, well-known technology, and usability in retrofit applications. The main drawbacks are related to their cost, their inability to store heat (peak-shave), and their low operating mean water temperature requiring thoughtful space dew point control to avoid condensation. TABS, usually fabricated as hydronic cross-linked

Received June 18, 2014; accepted March 12, 2015

**Stefano Schiavon, PhD, PE**, Associate Member ASHRAE, is an Assistant Professor. **Fred S. Bauman, PE**, Member ASHRAE, is a Project Scientist. **Brad Tully, PEng**, Associate Member ASHRAE, is a General Manager. **Julian Rimmer, PEng**, Member ASHRAE, is the Vice President, Design and Business Development.

\*Corresponding author e-mail: stefanoschiavon@berkeley.edu

Color versions of one or more of the figures in the article can be found online at [www.tandfonline.com/uhvc](http://www.tandfonline.com/uhvc).

polyethylene (PEX) tubing embedded in slabs, are less expensive than radiant panels, have the ability of peak shaving and shifting, are fast to answer to heat gains, and usually operate at higher cooling temperatures, reducing the condensation risk and increasing energy performance. The main drawbacks are related to the complexity of the design and control and the slow response of the thermally massive slab to control signal changes (Lehmann et al. 2007).

Alamdari et al. (1998) described how adding a CC to a DV system influences the air distribution characteristics of DV. Rees and Haves (2001) developed a nodal model to represent room heat transfer in DV and CC systems that is suitable for implementation in an annual energy simulation program but cannot be applied as a stand-alone design tool. Novoselac and Srebric (2002) did an extensive critical literature review of the performance and design of a combined CC and DV system and concluded that one of the key parameters of the design is the cooling load split between the CC and DV system. Tan et al. (1998) defined  $\eta$  as the ratio of the zone cooling load removed by the CC ( $CL_{CC}$ ) to the total room cooling load ( $CL$ ).  $\eta$  may vary between 0 and 1. If  $\eta$  equals 1, it means that a pure CC system is used; on the other hand, if  $\eta$  equals 0, a pure DV system is used. Tan et al. (1998) suggested that to maintain a temperature gradient of at least 2 K/m, the DV system should remove a minimum of 33% of the cooling load (i.e.,  $\eta = 0.67$ ). Behne (1999) stated that good thermal comfort and air quality could be maintained when the DV system removes at least 20%–25% of the total cooling load.

Ghaddar et al. (2008) developed general design charts for sizing the CC/DV systems using a model developed by Ayoub et al. (2006). The main limitation of the method is related to the fact that the design charts were developed for a 100% ceiling coverage ratio and by using the ratio of the zone cooling load removed by the CC to the total room cooling load (why this is an issue is later described). Sensitivity analysis has been performed for 80% ceiling coverage ratio; there are no data for lower ceiling coverage ratio. The ceiling coverage is the ratio, expressed as a percentage, of active radiant area to the total ceiling area. According to the authors' experience for metal radiant panels, the typical installed ceiling coverage in the United States varies between 40% and 60%. Keblawi et al. (2009) expanded Ghaddar et al. (2008) to operating sensible load ranges from 40 to 100 W/m<sup>2</sup>. The model relates system load and operational parameters with comfort measured by vertical temperature gradient and indoor air quality measured by the stratification height. Kanaan et al. (2010) developed and experimentally tested a simplified model to predict carbon dioxide transport and distribution in rooms conditioned by CC and DV. Chakroun et al. (2011) extended and validated the model to transient conditions and applied it to study the energy savings potential during the cooling season for a simplified room (25 m<sup>2</sup>) located in the Kuwait climate. To perform the energy simulation, they used an algorithm developed internally to their research group.

Schiavon et al. (2012) experimentally investigated the influence of percentage of ceiling active area and of the split of cooling load between displacement and CC on stratification. It was found that the average radiant ceiling surface temperature is a better predictor of the temperature difference

between the head (1.1 m) and ankle (0.1 m) of a seated person in the occupied zone compared to other parameters related to the fraction of the total cooling load removed by the radiant CC. This result accounts for the fact that when smaller active radiant ceiling areas are used (e.g., for a typical radiant ceiling panel layout), colder radiant surface temperatures are required to remove the same amount of cooling load (as a larger area), which cause more disruption to the room air stratification. It was also found that the room air stratification in the occupied zone (1) decreases as a larger portion of the cooling load is removed by the CC, (2) increases with higher radiant ceiling surface temperatures, and (3) decreases with an increase in the ratio between the total cooling load and the displacement airflow rate. These results confirmed those summarized by Novoselac and Srebric (2002). It was concluded that despite the impact that the CC has on stratification, the results indicate that a minimum head–ankle temperature difference of 1.5 K in the occupied zone (seated or standing) will be maintained for all radiant ceiling surface temperatures of 18°C or higher. These results were obtained for a cooling load of 34.7 W/m<sup>2</sup>. To the best knowledge of the authors, there are no published laboratory or field studies for a high cooling load.

Ventilation effectiveness is an indicator of the efficiency with which fresh air is delivered to the breathing zone in ventilated rooms, and it is related to indoor air quality. It is a representation of how well a considered space is ventilated compared to a uniform well-mixed room (Rim and Novoselac 2010). A detailed description of ventilation effectiveness can be found in ASHRAE (2002). In the United States, ventilation effectiveness is measured with the index called air change effectiveness (ACE) according to ASHRAE Standard 129–2002 (ASHRAE 2002). However, Rim and Novoselac (2010) questioned the overall ability of ACE as an indicator of air quality and human exposure. With climatic chamber experiments and a calibrated computational fluid dynamics (CFD) model, they showed that for fine particles (1  $\mu$ m), an increase in ACE reduces occupant exposure, while for coarser particles (7  $\mu$ m), source location and airflow around the pollutant source are the major variables that affect human exposure. It is important to keep these findings in mind with the application of DV, where pollutant sources located at floor level near an occupant could be drawn up to the breathing level by the rising thermal plume. Schiavon et al. (2011) reported three ACE tests and concluded that ACE higher than one is maintained in the occupied zone even when more than half (54%) of the heat load is removed by a CC and the radiant surface temperature is 18.7°C.

A group of HVAC designers working on a large headquarters for a multi-national corporation asked about the thermal comfort and indoor air quality performance of combined CC and DV system solution for a high cooling load (roughly 90 W/m<sup>2</sup>). As described above, sufficient information was not found in the existing literature, so a decision was made to perform a laboratory study. Increasing thermal stratification may reduce energy use, and it is well known from the literature that stratification profiles in DV systems can be significantly influenced by the type and location (height) of heat sources in the room (Skistad et al. 2002). To assess the magnitude of the po-

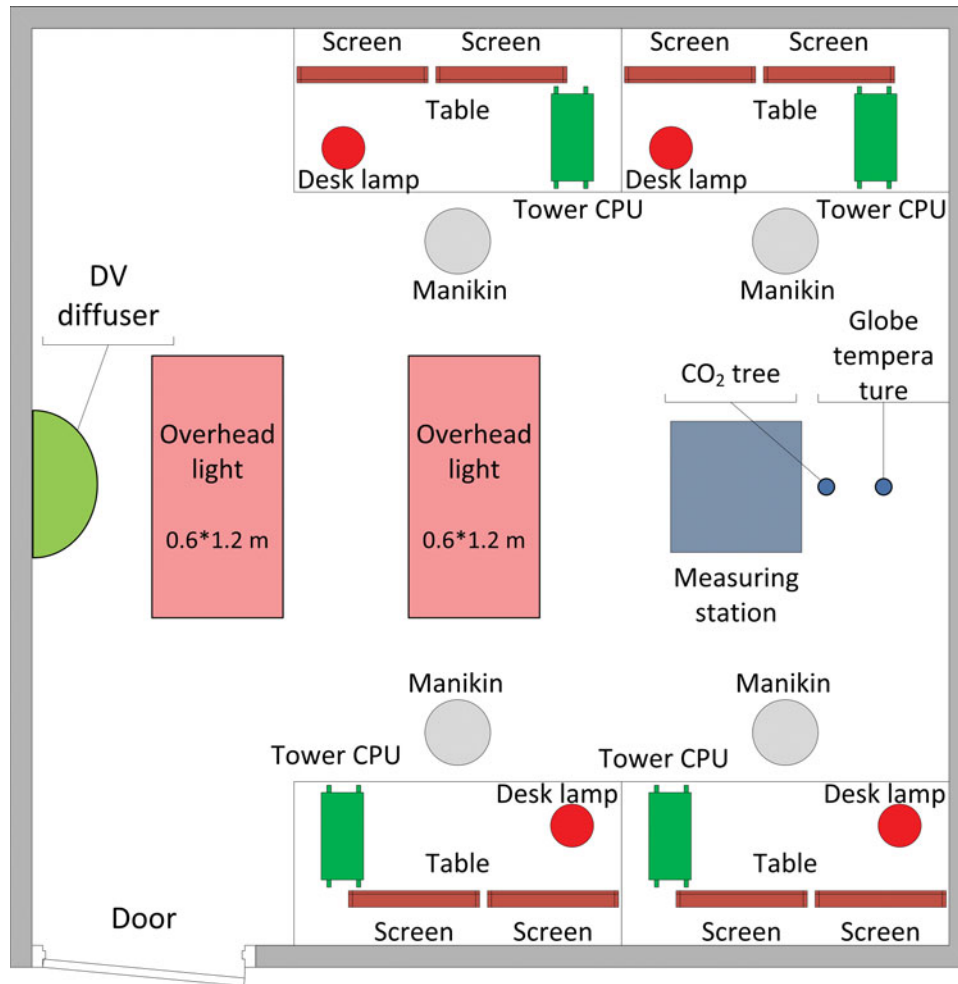


Fig. 1. Layout of test chamber.

tential beneficial impacts on comfort and energy performance of a room conditioned by DV with CCs, experiments were conducted to study a practical example of moving computer processing units (CPUs) from the floor up to a shelf at 1.52 m height.

The purpose of this study is to conduct laboratory experiments for a U.S. interior zone office with a high cooling load ( $91.0 \text{ W/m}^2$ ) and with two different heat source heights, represented by computer cases (at floor level and at 1.52 m), to investigate their influence on room air stratification and ACE. The zone is conditioned by a combined CC and DV system.

## Method

### *Experimental facilities and room description*

The experiments were carried out in a climatic chamber ( $4.27 \text{ m} \times 4.27 \text{ m} \times 3.0 \text{ m}$ ) equipped with radiant panels located in a suspended ceiling placed at a height of 2.5 m above the floor. The climatic chamber is located within a large conditioned laboratory space. The floor area of the climatic chamber is  $18.2 \text{ m}^2$ , and the volume is  $54.7 \text{ m}^3$ . The room has

no windows. The walls, the ceiling, and the floor have similar construction and thermal properties. Starting from the exterior, the chamber wall is comprised of  $3.522 \text{ m}^2\text{K/W}$  insulation, a stagnant  $0.102 \text{ m}$  air gap ( $0.352 \text{ m}^2\text{K/W}$ ), aluminum extruded walls, and another layer of  $0.102 \text{ m}$  of polyurethane board ( $3.522 \text{ m}^2\text{K/W}$ ). By adding up this assembly, the overall conductance is  $0.135 \text{ W/m}^2\text{K}$ .

Each aluminum radiant panel installed in the suspended ceiling was  $1.83 \text{ m}$  long and  $0.61 \text{ m}$  wide (area equal to  $1.11 \text{ m}^2$ ). Copper pipes are thermally connected to aluminum channels in panels with a spacing of  $0.15 \text{ m}$  (Price Radiant Panel RPL). The suspended ceiling is composed of radiant ceiling panels connected in series. Cotton fiber insulation was present over the panels ( $2.288 \text{ m}^2\text{K/W}$ ). Twelve panels were centrally positioned in the ceiling, covering  $73.5\%$  ( $13.4 \text{ m}^2$ ) of the total area. The ceiling coverage factor is higher than typical U.S. values because the investigated cooling load was high, and interest was to investigate the performance of TABS, which would always have a high coverage factor. Figure 1 shows the locations of the four simulated workstations, office heat loads, measuring station for recording the vertical temperature profile,  $\text{CO}_2$  measuring tree, and location of the globe thermometer. The inlet air was supplied to the room from a

**Table 1.** Heat load summary.

Heat source	Number	Power per unit (W)	Total power (W)	Power per floor area (W/m <sup>2</sup> )
CPUs	4	212	848	46.6
Screens and lamps	8	44.25	354	19.5
People	4	75	300	16.5
Instrument tree and datalogger	1	20	20	1.1
Overhead lighting	2	67.5	135	7.4
Total			1657	91.0

1.2-m-tall semi-circular wall-mounted displacement diffuser (radius = 0.6 m). Heat sources are summarized in Table 1. Office heat sources were modeled using tower CPUs (sometimes referred to as PCs, or personal computers, or computer cases; the terms CPUs and computer cases are used interchangeably herein), representing 51% of the total heat gain, flat screens and desk lamps on the desks, and overhead lighting. A portion (36%) of the heat gains generated by the tower CPUs was generated with electrically heated 0.35-m-by-0.35-m galvanized steel plates there were not enough tower CPUs. The plates (2 mm thick) are heated by two silicon rubber strip heaters mounted with high-temperature room temperature vulcanizing adhesive. The convective/radiative split and surface temperature of these plates are similar to those of tower computers. Occupants were simulated with heated thermal manikins according to EN 14240 (European Committee for Standardization [CEN] 2004). These simulators represent a load on the space by using light bulbs enclosed in a sheet metal cylinder. They try to match the radiant convective split of a person by using high-emissivity paint and holes to allow air to pass through. When fully installed, the test chamber represented a four-person office with multiple computers (high heat gain) at each workstation.

### Measuring instruments and uncertainty

The same test facility and instrumentation were used as described in Schiavon et al. (2012). A detailed description of the sensors and their measurement uncertainty is reported there. The data are analyzed in accordance with the Joint Committee for Guides in Metrology (JCGM) guideline (2008) for the expression of uncertainty. The sample uncertainty of the derived quantities (air and water temperature differences, cooling load removed by the panels, electrical load, and  $\eta$  [see definition below]) has been evaluated. The derived uncertainty of the air temperature difference is  $\pm 0.41$  K, the water temperature difference is  $\pm 0.125$  K, the cooling load removed by the CC is  $\pm 25.5$  W, the electrical total power is  $\pm 14.7$  W, and  $\eta$  is  $\pm 0.04$ . When presented, the uncertainty is indicated by means of error bars. The level of confidence is 95% (coverage factor 2).

Carbon dioxide (CO<sub>2</sub>) was used as the tracer gas for ACE measurements. CO<sub>2</sub> was measured with a Vaisala CARBOCAP Carbon Dioxide Transmitter GMP222. All CO<sub>2</sub> probes were calibrated using a two-point calibration method using the Vaisala GMK220. The first point was measured at 0 ppm of CO<sub>2</sub>, and the second point was measured at 5050 ppm of CO<sub>2</sub>. The new calibration data was uploaded to each individual probe, and a spot check was done using 2460 ppm CO<sub>2</sub>. CO<sub>2</sub> sensors were located in the supply diffuser in the exhaust and at three heights in the room (0.6, 1.1, and 1.7 m) at the CO<sub>2</sub> sensor tree (see Figure 1). The step-up method according to ASHRAE Standard 129–2002 (ASHRAE 2002) was used and the measurements comply with its requirements. Data were collected with a National Instruments data acquisition system.

### Experimental conditions and procedure

$\eta$  ( $\eta$ ) is the ratio of the cooling load removed by the CC,  $CL_{CC}$ , over the total cooling load and is expressed by the following equation:

$$\eta = \frac{\text{cooling load removed by CC}}{\text{total cooling load}} = \frac{CL_{CC}}{CL_{DV} + CL_{CC}} \quad (1)$$

The total cooling load is equal to the electrical power of the heat sources because the measurements were done in steady-state conditions and the external gains through the chamber walls are negligible; thus, the heat gains are equal to the cooling loads. The cooling load removed by the radiant panels  $CL_{CC}$  has been calculated with the following formula:

$$CL_{CC} = m_w c_{p,w} (t_{w,r} - t_{w,s}), \quad (2)$$

where  $c_{p,w}$  is the specific heat capacity of water. The cooling load removed by DV,  $CL_{DV}$ , was calculated indirectly as the difference between the total cooling load and the cooling load removed by the radiant ceiling panels. The cooling load removed by DV could also be calculated directly by measuring the airflow rate and the supply and return air temperature. This procedure was not used because the accuracy of the water flow sensor was much higher than that of the airflow rate sensor.

The experiments are summarized in Table 2. The experiments are identified based on a first-order estimation of the airflow rate measured in L/s, the temperature set-point (24 or NC, where NC stands for “not constrained,” meaning that the set-point is not fixed), and the location of the heat sources (F stands for “floor;” and H stands for “at 1.52 m height above the floor). The heat load in the room was kept constant and equal to 1657 W (91.0 W/m<sup>2</sup>). The heat loads are described in Table 1. The operative temperature,  $t_{op}$ , was kept constant and almost equal to 24°C, except in tests 140-NC-H and 75-NC-H. The operative temperature was calculated as the average of the mean radiant temperature (0.6 m height) and the average seated air temperature according to the International Organization for Standardization’s (ISO) ISO 7726 Annex G (1998). In these experiments, air velocity was not measured because

**Table 2.** Experimental tests summary.

Test	Airflow rate (L/s)	$\eta^a$	Operative temperature (°C)	CPUs location
180–24-F	181.4	0.20	24	Floor
160–24-F	163.2	0.24	24	Floor
140–24-F	138.2	0.47	24	Floor
120–24-F	117	0.57	24	Floor
95–24-F	94.5	0.64	24	Floor
75–24-F	72.4	0.73	24	Floor
35–24-F <sup>b</sup>	36.6	0.89	24	Floor
130–24-H	131.6	0	24	At 1.52 m
100–24-H	102.3	0.34	24	At 1.52 m
75–24-H	74.4	0.57	24	At 1.52 m
140-NC-H	142.2	0.49	Not constrained	At 1.52 m
75-NC-H	75.3	0.75	Not constrained	At 1.52 m

<sup>a</sup>This parameter was calculated after performing the experiment.

<sup>b</sup>The total power was 1803 W and not 1657 W, as in the other experiments, because an extra pump had to be added in the room above the radiant panels to increase their water flow rate. In the calculation of  $\eta$ , the power of the pump was included; if the pump was not included, then  $\eta$  would have been equal to 0.97. For this test, it was not possible to perform the ACE test due to time constraints.

it was previously found that the air velocity measured at 0.6, 1.1, and 1.7 m was not affected by the DV airflow rate, and it was always lower than 0.10 m/s. The used operative temperature calculation method is valid only when the air velocity is lower than 0.2 m/s (ISO 1998). The average seated air temperature was the mean value of the air temperatures measured at 0.1, 0.6, and 1.1 m. In a stratified environment, there is no single height where the air temperature can be measured that represents the “perceived” air temperature. For this reason, the average of the air temperatures measured at ASHRAE Standard 55–2013 (ASHRAE 2013a) heights was used. DV supply air temperature  $t_{air,s}$  was kept constant and equal to 18°C. To keep the operative temperature set-point equal to 24°C, the water mass flow rate and cold water supply temperature were manually adjusted; turbulent flow conditions were always maintained, and an attempt was made to keep the water temperature difference (return and supply) between 1 and 3 K. In experiments 140-NC-H and 75-NC-H, the air and water flow rates and the supply air and water temperatures were kept constant and equal to cases 140–24-F and 75–24-F to study the influence on the ACE and thermal stratification of just moving the computer heat sources to a higher part of the room. When the CPUs were located at the floor level, seven airflow rates were tested to have a wide range of cooling load splits between DV and the CC. Due to time and budget constraints, a reduced number of airflow rates was tested for the cases with part of the heat gains located at 1.52 m. The air, water, and globe temperatures, cooled water mass flow rate, and airflow rate were recorded for at least 30 min after steady-state conditions were obtained. The electrical power consumption was manually recorded before starting the experiments.

The computer cases (CPUs) are equal to 51% of the total heat gains and 71% of the heat gains coming from the office equipment (screen and CPUs). Screens cannot be moved from the desk, but the location of the CPUs is flexible. They are often located on the floor under the desk. Two locations were tested: the first (named floor or F) in which the tower CPUs were located at floor level under the desk and the second in which they were placed on open shelves above the desks 1.52 m (5 ft) above the floor.

The tests summarized in Table 2 were performed in June 2012. In the results and discussion sections, results from previous CC/DV testing in the same lab will also be reported (Schiavon et al. 2012). To verify consistency between separate lab tests, the experiment without radiant panels (only DV) was repeated and compared for all visits. The temperature profiles were found to be very similar. The average of air temperature differences between the cases calculated at each height was 0.30 K.

## Results and discussion

The main performance parameters of the DV and CC systems obtained in the experiments are summarized in Table 3. The operative temperature for the first ten experiments was controlled within the range of 24.0°C–24.2°C; therefore, it may be concluded that the comparison was done with almost thermally equal comfort conditions. The DV supply air temperature was precisely controlled at 18°C. The airflow rate varied between 36.6 to 181.4 L/s (2.4–11.8 air changes per hour).

### Temperature stratification

The vertical air temperature profiles are shown in Figure 2. Figure 2a shows the temperature stratification when the PCs are located at the floor level below the desks. From Figure 2a, it can be deduced that the temperature stratification in the occupied zone for a seated person (up to 1.1 m height) is not strongly affected by the change in the cooling load split between DV and the CC. The stratification is reduced from 2.1 to 0.8 K when the airflow is reduced from 181.4 to 36.6 L/s ( $\eta = 0.20$  to 0.89). At higher heights in the room, it can be seen that temperature stratification is reduced as the amount of load removed by the CC increases. The suspended ceiling is located at 2.5 m from the floor. Figure 2 reports the air temperatures from the floor to the suspended ceiling; between the suspended ceiling and the exhaust there is a void space. When the panels are activated, i.e., cooled, exhaust air  $t_{air,r}$  is cooler than the temperature measured at 2.4 m by the panels. Figure 2a shows that most of the temperature stratification is occurring in the occupied zone. The relatively well-mixed conditions (small temperature differences) at higher heights in the room is a good indication that these points fall above the stratification height that separates the two characteristic lower and upper zones of a stratified DV system. Experiment 35–24-F was not fully successful. The aim of this experiment was to test the combination of DV and CC in extreme conditions, with the CC taking almost 90% of the load and providing only

**Table 3.** Experimental performance parameters.

Test	$\eta$	$t_{op}$ (°C)	Displacement		Radiant panels					
			$V_{air}$ (L/s)	$t_{air,r}$ (°C)	$m_w$ (kg/h)	$t_{w,r}-t_{w,s}$ (K)	$t_{w,m}$ (°C)	$CL_{CC}$ (W)	$CL_{CC}^a$ (W/m <sup>2</sup> )	$CL_{CC}^b$ (W/m <sup>2</sup> )
180–24-F	0.20	24.0	181.4	23.9	200	1.4	22.8	324	24	18
160–24-F	0.24	24.0	163.2	23.7	150	2.3	21.8	397	30	22
140–24-F	0.47	24.1	138.2	23.3	283	2.4	18.3	779	58	43
120–24-F	0.57	24.0	117.0	23.1	400	2.0	16.8	937	70	51
95–24-F	0.64	24.0	94.5	23.3	419	2.2	15.4	1069	80	59
75–24-F	0.73	24.0	72.4	23.1	400	2.6	14.1	1206	90	66
35–24-F	0.89	24.0	36.6	23.5	575	2.4	10.9	1605	120	88
130–24-H	0.00	24.1	131.6	27.8	0	2.0	26.2	0	0	0
100–24-H	0.34	24.0	102.3	26.2	283	1.7	24.7	564	42	31
75–24-H	0.57	24.2	74.4	25.1	400	2.0	20.7	937	70	51
140-NC-H	0.49	21.2	142.2	22.8	283	2.5	18.3	813	61	45
75-NC-H	0.75	21.4	75.3	22.0	400	2.7	14.1	1237	92	68

<sup>a</sup>Panel capacity expressed per unit of panel area.

<sup>b</sup>Panel capacity expressed per unit of floor area.

36.6 L/s (that is a bit more than double of the minimum outdoor airflow rate [15.5 L/s] according to ASHRAE 62.1–2013 [ASHRAE 2013b] for an office space). To obtain the operative temperature equal to 24°C, the water supply temperature was reduced to 9.7°C (mean water temperature was 10.9°C), which is too low for almost any real application. Even at 9.7°C, the desired operative temperature could not be obtained, and the mass flow rate was increased from 419 to 575 kg/h; to do this, an extra pump was added in the room, above the radiant panels. The obtained temperature profile was correct, but an ACE test could not be performed due to time constraints.

Figure 2b shows the temperature stratification when the PCs are located at 1.52 m above the floor. The effect is dramatic. After a lower layer from 0 to 0.6 m, where the air is relatively well mixed, there is a strong stratification between 0.6 and 1.7 m. There are two groups of profiles. Those on the left (dotted lines) when the temperature in the room was allowed to fluctuate, and the group with solid lines where the average operative temperature in the occupied zone was maintained at 24°C.

In only two cases (100–24-H and 75–24-H) was the vertical temperature difference between head (1.1 m) and ankle (0.1 m) for seated occupancy observed to exceed 3 K, the maximum acceptable stratification specified by ASHRAE Standard 55–2013 (ASHRAE 2013a). According to ASHRAE Standard 55–2013 (ASHRAE 2013a), the vertical temperature difference between head (1.7 m) and ankle (0.1 m) for a standing occupant should not exceed 4 K. For cases 100–24-H, 140-NC-H, and 75–24-H, this threshold was exceeded. In all these cases, the CPUs were in the higher part of the room. CC/DV systems even with high cooling loads are able to maintain stratification lower than 3 K, if more than 50% of the heat gains are in the lower part of the room. In applications of CC/DV to spaces with stratification approaching 3 K, it is advisable to remove a high enough percentage of the total load by the CC to maintain stratification at acceptable levels.

Lower stratification (0.8 K) was obtained for the experiment 35–24-F when  $\eta$  was equal to 0.89 and  $t_p$  was equal to 10.9°C.

Figure 3 compares the temperature profiles of three tests: 75–24-F, 75-NC-H, and 75–24-H. In all these tests, the heat gains (91.0 W/m<sup>2</sup>), airflow rate (~74 L/s), and air supply temperature have been held constant. From test 75–24-F to 75-NC-H, the only thing changed was the location of the CPUs (airflow rate, water flow rate, and supply water temperature were kept constant), and this caused the variation of the temperature profile. From under the desk at floor level, the CPUs, representing 51% of total heat gains and 71% of heat gains from the office equipment, were moved above the desk to 1.52 m above the floor. The effect on average temperature in the occupied zone and the amount of stratification are significant. The temperature at ankle level is reduced from 23°C to 20.7°C and at 1.1 m from 24.7°C to 23.2°C. This air temperature reduction produces a decrease in operative temperature equal to 2.6 K (from 24°C to 21.4°C). The temperatures at the ceiling height are quite similar for these two tests. To compare the effect of moving the CPUs from the floor to 1.52 m height on energy use, a third test (75–24-H) was performed at similar thermal comfort conditions to the original floor-level load test (75–24-F). To accomplish this, the supply water temperature to the radiant panels was progressively increased from 12.8°C to 19.7°C. This implied that the average water temperature increased from 14.1°C to 20.6°C. An operative temperature of 24.2°C was obtained, almost equal to case 75–24-F.

Note that for both tests with the increased height of the CPUs (75-NC-H and 75–24-H), there is a noticeable jump in temperature gradient at the 1.7 m height (lower than expected). Two reasons for this observed pattern are suspected: (1) the 1.7 m temperature sensor is located close to or slightly above the interface layer separating the lower and upper zones established by the DV airflow distribution; room temperatures in this layer could be subject to mixing and (2) it is not sur-



prising that the large amount of heat gain added to the room at a height above 1.7 m (the tops of the CPU units extend to a height of approximately 2 m) causes an increase in temperature near the ceiling.

It can be concluded that increasing the height of the heat sources from the floor to about head height for the same thermal comfort conditions allows a significant increase in radiant panel surface temperature, thereby saving cooling energy. This simple strategy has strong potential for reducing energy consumption in stratified systems (DV and UFAD), as well as implementation of passive or renewable energy sources, such as cooling tower, ground source heat pumps, etc. It is interesting to notice that an increase temperature stratification may also change the amount of infiltration/exfiltration and the total heat transfer through the building envelop.

**ACE**

ACE tests were performed for 11 of the 12 tests (35–24-F was not performed). Figure 4a presents a representative example of the measured CO<sub>2</sub> concentrations versus time for test 180–24-F. Measurements are reported for supply, exhaust, and

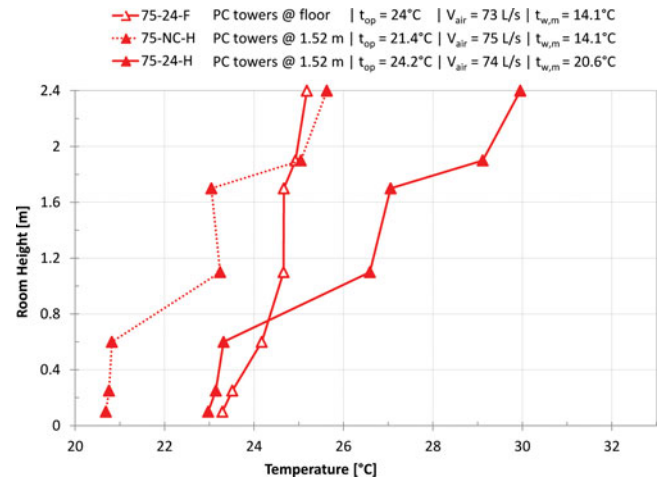


**Fig. 3.** Temperature profiles for 75-24-F, 75-NC-H and 75-24-H. Heat gains, airflow rate and supply air temperature were constant. From 75-H-F to 75-NC-H only the CPUs location was changed. From 75-NC-H to 75-24-H only the water temperature supplied to the radiant panels was increased.

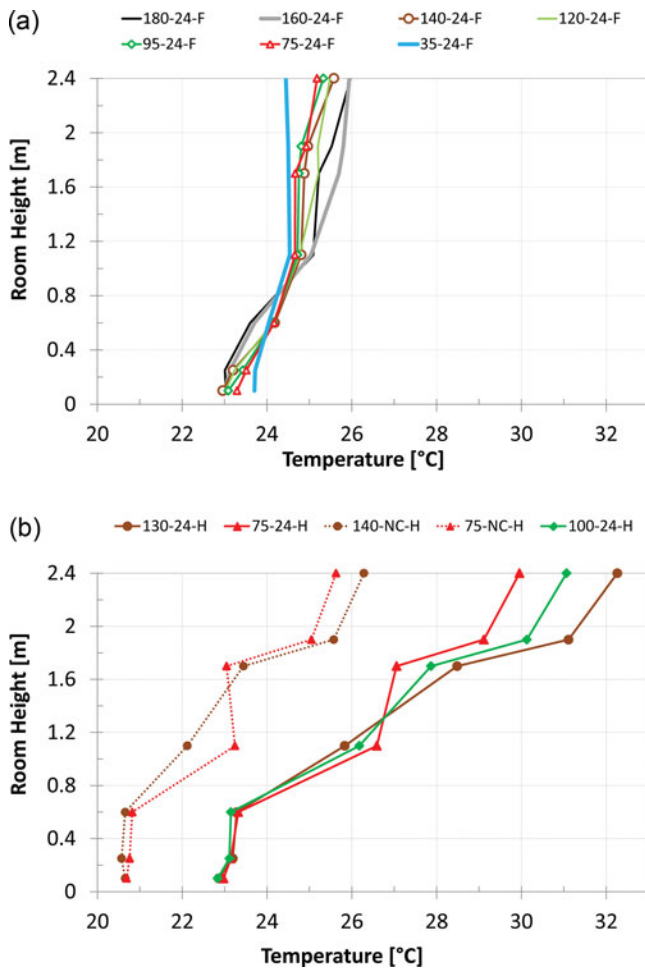


**Fig. 2.** Air temperature profiles for twelve tests described in Table: (a) tests with the CPUs located at floor level; and (b) tests with CPUs located at 1.52 m height above floor.

three heights in the room (0.6, 1.1, and 1.7 m). The observed constant final CO<sub>2</sub> concentrations achieved at all locations are a good indication that the requirements of the step-up tracer gas measurement method were met. The reported concentrations have been adjusted with respect to the average background (outdoor) concentration. Figure 4b presents a representative example of the calculated ACE for the three heights versus time for test 180–24-F. Note that the calculated ACE values (read on the left-hand axis) exhibit classic DV behavior with higher values at lower heights and all values greater than one. The variability in ACE values is the result of the calculation process involving measured concentrations that are approaching the same value over time. The ACE values calculated at 0.6, 1.1, and 1.7 m and three key performance parameters of the DV and CC systems are summarized for all completed tests in Table 4.

The median ACE at 0.6 m is 2.3 (maximum = 3.2 and minimum = 1), the median ACE at 1.1 m is 1.5 (maximum = 2.1 and minimum = 1), and the median ACE at 1.7 m is 1.2 (maximum = 1.4 and minimum = 0.9). All the ACE median values are higher than one (mixing ventilation). Among the parameters reported in Table 4, the height of the heat sources has the strongest effect. When the heat sources are located in the higher part of the room, ACE at 0.6 m is consistently higher than 2, ACE at 1.1 m equals 1.6 on average, and ACE at standing head height (1.7 m) is nearly equal to a constant, 1. This means that if the heat sources are located in the higher part of the room, two separate zones can be created, one of clean and fresh air in the lower part of the room (seated occupants) and one with warmer mixed air in the higher part of the room. For the same heat source location, the ACEs at 0.6 m and 1.1 m increase with increasing airflow rate, decreasing  $\eta$ , and increasing panel surface temperature.

**Table 4.** ACE results.

Test	Calculated $\eta$ (—)	Panel surface temperature ( $^{\circ}\text{C}$ )	$CL/V_{air}$ ( $\text{kW}/(\text{m}^3/\text{s})$ )	ACE at 0.6 m (—)	ACE at 1.1 m (—)	ACE at 1.7 m (—)
180–24-F	0.20	22.8	9.1	2.3	1.9	1.3
160–24-F	0.24	21.8	10.2	1.8	1.5	1.4
140–24-F	0.47	18.3	12.0	1.1	1.2	1.2
120–24-F	0.57	16.8	14.2	1.0	1.1	1.3
95–24-F	0.64	15.4	17.5	1.1	1.2	1.3
75–24-F	0.73	14.1	22.9	1.2	1.3	1.4
130–24-H	0.0	26.2	12.6	2.7	2.1	0.9
100–24-H	0.34	24.7	16.2	2.9	1.7	0.9
75–24-H	0.57	20.7	22.3	3.2	1.5	1.0
140-NC-H	0.49	18.3	11.7	2.6	1.8	0.9
75-NC-H	0.75	14.1	22.0	2.9	1.0	1.2
Maximum				3.2	2.1	1.4
Minimum				1.0	1.0	0.9
Average				2.1	1.5	1.2
Median				2.3	1.5	1.2

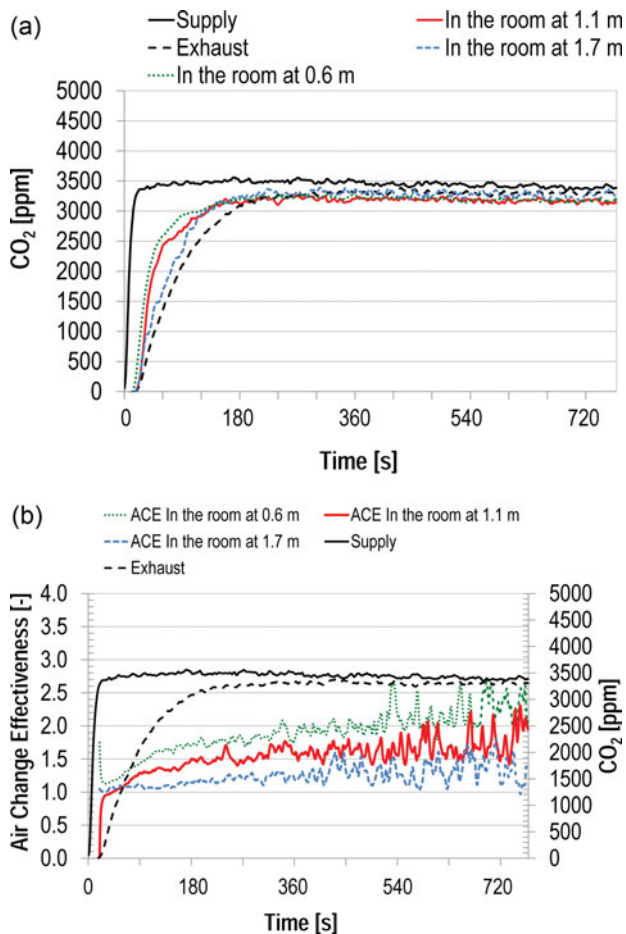


**Fig. 4.** (a) CO<sub>2</sub> concentrations for the step-up method at the supply, exhaust and at 0.6, 1.1 and 1.7 m for test 180-24-F; (b) Air change effectiveness calculated at 0.6, 1.1, and 1.7 m and CO<sub>2</sub> concentrations for the supply and exhaust for test 180-24-F.

### Prediction models based on combined database

The data analyzed in this article have been obtained from the same climatic chamber previously described by Schiavon et al (2012). It is therefore possible to compare and merge the two datasets. This was done to build a more robust design model that can be applied over a wider range compared to the two separate databases.

In this section, the terms “mean water temperature” and “radiant surface temperature”,  $t_p$ , are synonymous, because in these tests with metal radiant panels, the two values were almost the same. This would not be correct for TABS. A model that could work for radiant panels and TABS must be developed; therefore, the present reference is the surface temperature of the radiant element.

Tan et al. (1998) and Ghaddar et al. (2008) stated that the ratio between total cooling load  $CL$  and displacement airflow rate  $V_{air}$  is relevant for prediction of the stratification in a room with DV and a CC. This article terms this ratio  $CL/V_{air}$ . Previously, it was demonstrated that the ratio of the cooling load removed by the CC over total cooling load  $\eta$  cannot be a unique parameter to predict the stratification, because cases with equal  $\eta$  may have different profiles when the active ceiling area is different (i.e., different ceiling coverage ratio). It was moreover found that the radiant surface temperature and  $CL/V_{air}$  are better predictors of the stratification than  $\eta$ . By looking at the new data,  $\eta$  was found to be strongly correlated to  $t_p$  (Spearman’s rank correlation coefficient,  $r = -0.83$ ) and to  $CL/V_{air}$  ( $r = 0.88$ ). This means that these parameters can be used instead of  $\eta$ . It is preferable to use  $t_p$  and  $CL/V_{air}$  because they are the physical parameters that affect the fluid dynamics in the space. A strong correlation between  $t_p$  and  $CL/V_{air}$  ( $r = -0.71$ ) was also found, which could imply that only one of the two parameters is needed as the independent variable in a predictive model.

Figure 5 presents air temperature differences between the head and ankle of a seated (1.1–0.1 m) occupant as function of the mean surface radiant panel temperature for data pre-

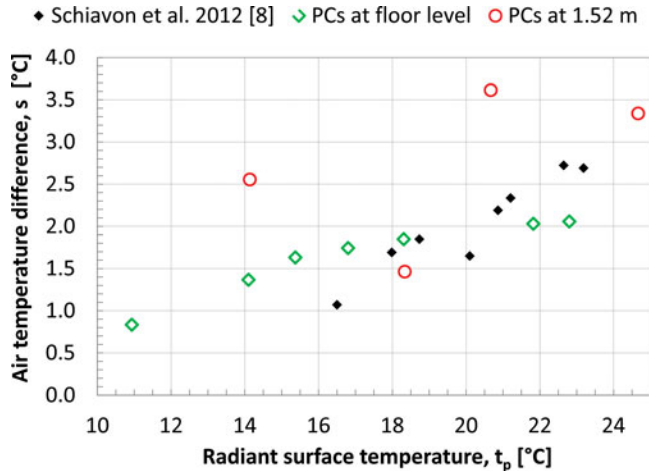


**Fig. 5.** Air temperature difference between head and ankle for seated occupant (1.1 – 0.1 m) as function of the radiant panel average surface temperature for previously published data (Schiavon et al. 2012) and the tests with the CPUs at the floor level and at 1.52 m.

viously published and tests reported in this article. Figure 6 shows the same temperature differences as a function of the ratio between the total cooling load and the displacement airflow rate. Figures 5 and 6 demonstrate that previously published data (Schiavon et al. 2012) and the present data obtained at high cooling load when the CPUs are located under the desk both exhibit similar behavior. It is therefore possible to merge the two datasets and develop a more robust regression model.

Four variables ( $t_p$ ,  $\eta$ ,  $CL/V_{air}$ , and a dummy variable that identifies if the CPUs are located in the lower or higher part of the room) were used to develop a predictive model. A multivariable regression linear model was developed. Regres-

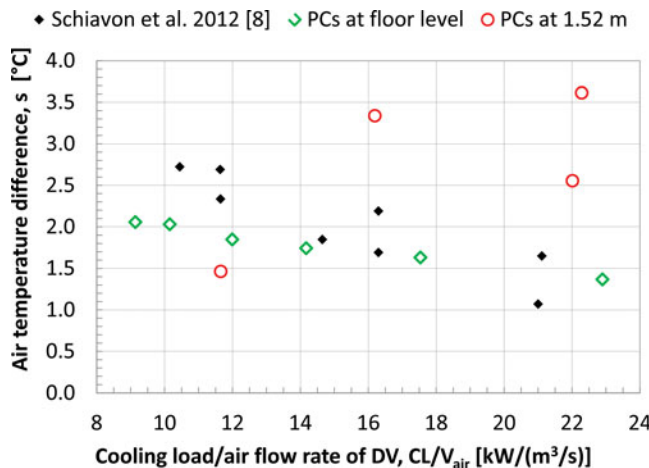


**Fig. 6.** Air temperature difference between head and ankle for seated occupant (1.1 – 0.1 m) as function of ratio between the total cooling load and the displacement air flow rate for previously published data (Schiavon et al. 2012) and the tests with the CPUs at the floor level and at 1.52 m.

sion models were selected based on  $R^2$  adjusted values and the authors’ judgment of the maximum number of useful explanatory variables.  $R^2$ , the coefficient of determination of the regression line, is defined as the proportion of the total sample variability explained by the regression model. Adding irrelevant predictor variables to the regression equation often increases  $R^2$ ; to compensate for this,  $R^2$  adjusted can be used.  $R^2$  adjusted is the value of  $R^2$  adjusted down for a higher number of variables in the model. Regression models are considered statistically significant when  $p < 0.05$ . The statistical analysis was performed with R version 2.15.3 (R Development Core Team 2013). All the data points have been used except those with pure DV ( $\eta = 0$ ). The best regression model, in SI and IP units, is reported as

$$SI : s = 0.127t_p - 0.528 + k_1, \quad (3)$$

$$I - P : s = 0.127t_p - 4.568 + k_2, \quad (4)$$

where  $s$  is the temperature difference between 1.1 and 0.1 m (43 and 4 in.) in °C (°F),  $t_p$  is the mean radiant panel surface temperature in °C (°F), and  $k_1 = 0.808$  and  $k_2 = 1.4544$  if at least 50% of the heat gains are located at 1.5 m (5 ft) or higher. The model is valid within the experimental conditions tested:  $10.9^\circ\text{C} (51.7^\circ\text{F}) < t_p < 24.9^\circ\text{C} (76.4^\circ\text{F})$ .

The analysis of variance (ANOVA) of the regression model indicated that the model is significant ( $p < 0.001$ ), the adjusted  $R^2$  is equal to 0.64, and the median of the residual is  $-0.01$  (first quartile is  $-0.236$ , the third quartile is  $0.233$ ). Visual evaluation of the plot of residuals indicated that the hypotheses of the linear regression model were met, and thus, the model is statistically valid. Thanks to the data reported in this article, the applicability of the model has been expanded from  $16.5^\circ\text{C} < t_p < 24.9^\circ\text{C}$  to  $10.9^\circ\text{C} < t_p < 24.9^\circ\text{C}$ . From Equations 3 and 4, it can be deduced that the stratification decreases when the surface temperature of the panel also decreases (larger percentage of cooling load removed by CC). For the same cooling load, ventilation, and thermal comfort conditions, it is possible to increase stratification by increasing the active radiant surface area because this would allow a higher surface temperature to be used. In design, this could be accomplished by employing a larger area (TABS) radiant slab with a DV system instead of a typically smaller-area radiant panel design. Stratification increases by 0.13 K for every degree increment of the radiant surface temperature. Moving at least 50% of the heat gains from the floor level to 1.5 m (5 ft) or higher produces an increment of the stratification of 0.8 K (1.44°F).

The developed regression model with the 95% confidence interval is shown in Figure 7 for the case with  $k_1 = 0$  (heat sources located at the floor level). The clear influence of the location of the CPUs on stratification is shown in Figure 8; the difference between the two locations of the CPUs is included in the regression model with constant  $k$ . When the heat sources are located in the higher part of the room, the stratification increase significantly.

In a similar way to the previous model, a regression equation was developed to predict the non-dimensional temperature measured at the floor level,  $\phi_{0.1}$ , expressed in Equation 5. In this case, all data points obtained with the CPUs located

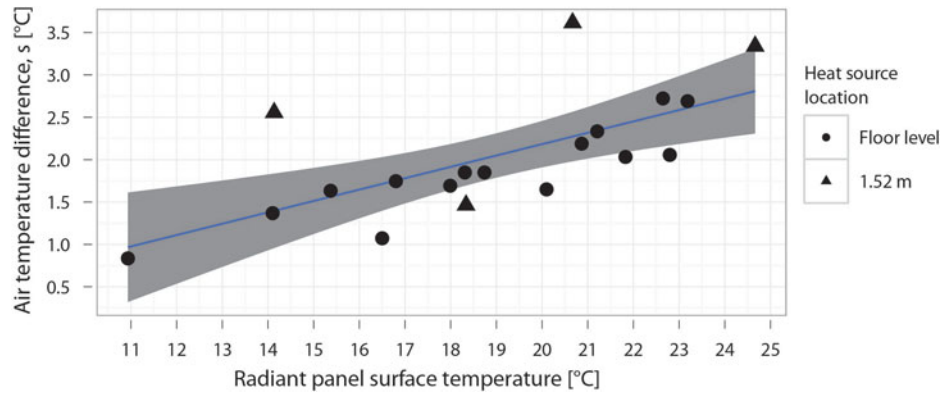


**Fig. 7.** Regression model of radiant panel surface temperature versus air temperature difference (Equation 3) with 95% confidence intervals.

at 1.52 m have been removed from the database because  $\phi_{0.1}$  was almost constant and equal to 0.35. In addition, the data-point obtained from test 35–24-F was removed because it was a leverage point for the regression:

$$\phi_{0.1} = \frac{t_{air,0.1} - t_{air,s}}{t_{air,r} - t_{air,s}}, \quad (5)$$

$$\phi_{0.1} = 0.0137 \frac{CL}{V_{air}} + 0.4748. \quad (6)$$

All variables used in Equations 5 and 6 are described in the nomenclature. The model is valid within the experimental conditions tested:  $9.1 \text{ kW}/(\text{m}^3/\text{s}) < CC/V_{air} < 22.9 \text{ kW}/(\text{m}^3/\text{s})$ .

The ANOVA analysis of the regression model indicated that the model is significant ( $p < 0.001$ ), and the adjusted  $R^2$  is equal to 0.73. Visual evaluation of the plot of residuals indicated that the hypotheses of the linear regression model were met, and thus, the model is statistically valid.

### ACE

When  $ACE > 1$  the designer, according to ASHRAE 62.1–2013 (ASHRAE 2013b), has the opportunity to reduce

the outdoor airflow rate or increase the indoor air quality with the same outdoor airflow. Table 4 shows that all ACE median values are greater than one. This implies that DV with a CC is able to provide better indoor air quality than a mixing ventilation system, even for an extremely high cooling load ( $91 \text{ W}/\text{m}^2$ ). In this research, ACE was measured at a location far from thermal plumes to have a fair representation of undisturbed contaminant concentration. For a seated occupant, even if the breathing zone is roughly at 1.1 m, he/she would breathe air taken from his/her own thermal plume originating from a lower level (e.g., 0.6 m). A moving occupant would most likely be exposed to the air at 1.1 m.

It was found that an ACE of 0.6 is strongly correlated with  $\phi_{0.1}$  ( $r = -0.74$ ), stratification  $s$  ( $r = 0.75$ ), and radiant panel surface temperature  $t_p$  ( $r = 0.43$ ). This means that if the stratification or panel surface temperature increases or  $\phi_{0.1}$  decreases, then the ACE of 0.6 increases. As also expected for this study characterized by high cooling loads, the higher the stratification is, the better the air quality is.

Figure 9 shows the boxplot of the ACE of 0.6 for the two CPU locations (floor level and at 1.52 m). Moving the CPUs from the floor to the higher part of the room increased markedly the ACE. Moving at least 50% of the heat gains from the floor to 1.52 m caused a median increase of the ACE measured at 0.6 m of 1.75 (from 1.15 to 2.90). Therefore, raising the height of the heat sources not only increases stratification but also improves indoor air quality ( $p < 0.001$ ). The spread (or inter quintile range) in Figure 9 for the tests with the heat

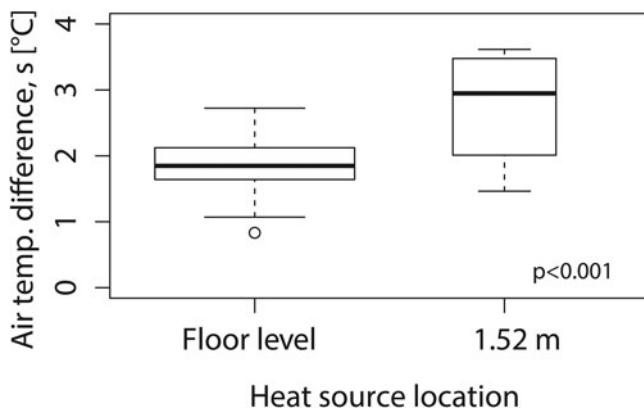


**Fig. 8.** Boxplot of the air temperature difference for the CPUs located at the floor level and at 1.52 m (high).

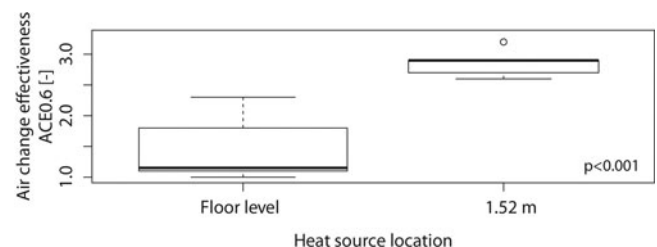


**Fig. 9.** Boxplot of the air change effectiveness measured at 0.6 m (ACE0.6) for the CPUs located at the floor level and at 1.52 m (high).

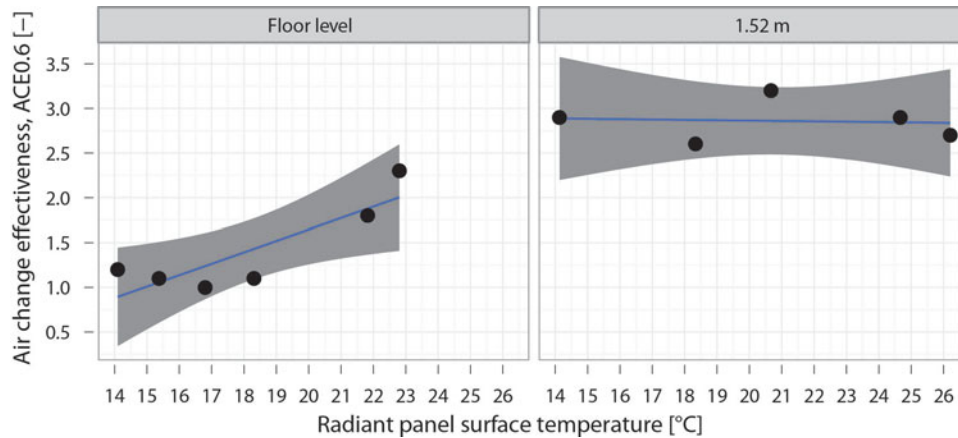


**Fig. 10.** Regression model of radiant panel surface temperature versus air change effectiveness measured at 0.6 m with 95% confidence intervals for the cases when the heat sources are located at the floor level (equation 7) and at 1.52 m (high).

sources located in the higher part of the room is very small. This implies that it is possible to summarize the data with the median and affirm that when the CPUs are located in the higher part of the room, an ACE of 0.6 is equal to 2.9. Figure 10 shows the regression models of radiant panel surface temperature versus ACE measured at 0.6 m with 95% confidence intervals for the cases when the heat sources are located at the floor level and at 1.52 m (high). For the former case (heat sources are located at the floor level), the regression equation to predict an ACE of 0.6 as a function of  $t_p$  is expressed in Equation 7. In this case, only six values from the dataset have been used, because either there were no ACE values or they were obtained for the CPUs located above the desks:

$$ACE_{0.6} = 0.13t_p - 0.9. \quad (7)$$

The model is valid within the experimental conditions values used for its development:  $14.1^\circ\text{C}$  ( $57.4^\circ\text{F}$ )  $< t_p < 22.8^\circ\text{C}$  ( $73^\circ\text{F}$ ). The ANOVA analysis of the regression model indicated that the model is significant ( $p < 0.028$ ), and the adjusted  $R^2$  is equal to 0.67. Visual evaluation of the plot of residuals indicated that the hypotheses of the linear regression model were met, and thus, the model is statistically valid.

The key finding from this study demonstrates that improved ACE (compared to a well-mixed system) is maintained in the lower occupied region of the room for a stratified DV system, even when 73% of the heat load is removed by a chilled radiant ceiling and the radiant panel surface temperature is higher than  $14.1^\circ\text{C}$ . Stratification and ACE both increase with the increase of the airflow rate, the decrease of  $\eta$ , and the increase of the panel surface temperature. It can be concluded that the higher the stratification is, the better the ACE will be.

### Limitations

These experiments did not directly calculate the uncertainty associated with ACE. Compliance with the standard was considered sufficient. The influence of exterior windows on air

distribution was not investigated. The experiments were performed in a test room representative of an interior zone with (almost) adiabatic walls. Under cooling conditions, it is possible that a rising thermal plume may develop close to warm exterior windows. There is no evidence of how this may affect the temperature stratification and the pollutant concentration. The proposed models based on the combined database are valid only within the boundary conditions reported in this article. Caution should be used if applied in perimeter zones. In this study, the influence of variations in supply air temperature, thermal comfort set-points, and heat source radiant/convective ratio has not been investigated. Latent loads were not simulated (heat was generated by thermal dummies), and humidity was not measured and controlled; this was outside the scope of these experiments. It is possible that the radiant surface temperatures for some test conditions could be lower than the dew point, and this should be considered in the design of the system.

### Conclusions

A laboratory experiment was conducted to investigate room air stratification in a typical office space with a combined radiant CC and DV system. The data collected in this experiment were merged with those described in Schiavon et al. (2012), and new prediction models have been developed. The main conclusions of this study follow.

- DV with a CC did not destroy thermal stratification for the range of test conditions investigated. The combined system was able to provide sufficient thermal stratification and improved ventilation efficiency in the occupied zone for a seated person compared to mixing ventilation, even for extremely high cooling loads ( $91 \text{ W/m}^2$ ).
- Stratification and ACE both decrease when the ceiling surface temperature also decreases (larger percentage of cooling load removed by a CC). For every degree decrement of the ceiling surface temperature, stratification decreases by 0.13 K and ACE by 0.13. Combining a larger active area radiant slab (TABS) with a DV system (instead of a

typically smaller active area radiant panel design) would allow higher radiant surface temperatures to be used, thus increasing stratification and improving ventilation performance.

- Employing a simple strategy of raising the height of the computer CPUs (representing 51% of total heat gain or 71% of office equipment heat gains) from the floor level to 1.5 m significantly increased stratification and the ACE measured at 0.6 m (from 1.15 to 2.90). Therefore, moving heat sources to a higher location in the room has the potential to reduce energy use and improve indoor air quality. When the computer CPUs were located at a height of 1.5 m in the room, the median stratification in the occupied zone for a seated person was 2.95 K.

### Nomenclature

$ACEX$	= air change effectiveness measured at $X = 0.6, 1.1,$ and $1.7$ m
$CC$	= chilled ceiling
$CL$	= total cooling load (W)
$CL_{CC}$	= cooling load removed by chilled ceiling (W)
$CL_{DV}$	= cooling load removed by displacement ventilation system (W)
$c_{p,w}$	= specific heat capacity of water (J/(kg K))
$DV$	= displacement ventilation
$m_w$	= water mass flow rate (kg/s)
$p$	= number of radiant ceiling panels
$s$	= air temperature stratification between 0.1 and 1.1 m (°C or K)
$t_{air,0.1}$	= air temperature measured at 0.1 m (°C)
$t_{air,r}$	= return air temperature from displacement ventila- tion system (°C)
$t_{air,s}$	= supply air temperature to displacement ventilation system (°C)
$t_{op}$	= operative temperature (°C)
$t_p$	= surface temperature of panel, here supposed equal to $t_{w,m}$ (°C)
$t_{w,m}$	= mean water temperature; average of $t_{w,s}$ and $t_{w,r}$ (°C)
$t_{w,r}$	= water temperature returned from chilled ceiling (°C)
$t_{w,s}$	= water temperature supplied to chilled ceiling (°C)
$V_{air}$	= airflow rate of displacement ventilation system (L/s)
$\eta$	= ratio of cooling load removed by chilled ceiling $CL_{CC}$ over total cooling load $CL$
$\phi_{0.1}$	= dimensionless air temperature measured at 0.1 m

### Acknowledgment

The authors would like to thank Tom Epp of Price Industries for his help in the laboratory testing.

### Funding

The present work was supported by the California Energy Commission (CEC) Public Interest Energy Research (PIER)

Buildings Program and in-kind contributions of laboratory facilities by Price Industries, Winnipeg, Manitoba.

### References

- Alamdari, F., D. Butler, P. Grigg, and M. Shaw. 1998. Chilled ceilings and displacement ventilation. *Renewable Energy* 15:300–5.
- ASHRAE. 2002. *ANSI/ASHRAE Standard 129–2002, Measuring Air-Change Effectiveness*. Atlanta: ASHRAE.
- ASHRAE. 2013a. *ANSI/ASHRAE Standard 55–2013, Thermal Environmental Conditions for Human Occupancy*. Atlanta: ASHRAE.
- ASHRAE. 2013b. *ANSI/ASHRAE Standard 62.1–2013, Ventilation for Acceptable Indoor Air Quality*. Atlanta: ASHRAE.
- Ayoub, M., N. Ghaddar, and K. Ghali. 2006. Simplified thermal model of spaces cooled with combined positive displacement ventilation and chilled ceiling system. *Science and Technology for the Built Environment* 12:1005–30.
- Behne, M. 1999. Indoor air quality in rooms with cooled ceilings: Mixing ventilation or rather displacement ventilation? *Energy and Buildings* 30:155–66.
- Causone, F., F. Baldin, B.W. Olesen, and S.P. Corgnati. 2010. Floor heating and cooling combined with displacement ventilation: Possibilities and limitations. *Energy and Buildings* 42:2338–52.
- Chakroun, W., K. Ghali, and N. Ghaddar. 2011. Air quality in rooms conditioned by chilled ceiling and mixed displacement ventilation for energy saving. *Energy and Buildings* 43:2684–95.
- Chen, Q., and L.R. Glicksman. 2003. *System performance evaluation and design guidelines for displacement ventilation*. ASHRAE, Atlanta.
- European Committee for Standardization (CEN). 2004. *Standard EN 14240–2004, Ventilation for Buildings—Chilled Ceilings—Testing and Rating*. Brussels, Belgium.
- Feng, J., F. Bauman, and S. Schiavon. 2014. Experimental comparison of zone cooling load between radiant and air systems. *Energy and Buildings* 84:152–9.
- Feng, J., S. Schiavon, and F. Bauman. 2013. Cooling load differences between radiant and air systems. *Energy and Buildings* 65:301–21.
- Feustel, H.E., and C. Stetiu. 1995. Hydronic radiant cooling—preliminary assessment. *Energy and Buildings* 22:193–205.
- Ghaddar, N., K. Ghali, R. Saadeh, and A. Keblawi. 2008. Design charts for combined chilled ceiling displacement ventilation system (RP-1438). *ASHRAE Transactions* 143:574–87.
- International Organization for Standardization (ISO). 1998. *International Standard ISO 7726, Ergonomics of the Thermal Environment—Instruments for Measuring Physical Quantities*. Geneva, Switzerland: ISO.
- Joint Committee for Guides in Metrology (JCGM). 2008. *JCGM 100, Evaluation of Measurement Data—Guide to the Expression of Uncertainty in Measurement*. Geneva, Switzerland; JCGM.
- Kanaan, M., N. Ghaddar, and K. Ghali. 2010. Simplified model of contaminant dispersion in rooms conditioned by chilled-ceiling displacement ventilation system. *Science and Technology for the Built Environment* 16:765–83.
- Keblawi, A., N. Ghaddar, K. Ghali, and L. Jensen. 2009. Chilled ceiling displacement ventilation design charts correlations to employ in optimized system operation for feasible load ranges. *Energy and Buildings* 41:1155–64.
- Leach, M., C. Lobato, A. Hirsch, S. Pless, and P. Torcellini. 2010. *Technical support document: Strategies for 50% energy savings in large office buildings*. National Renewable Energy Laboratory, Golden, CO.
- Lehmann, B., V. Dorer, and M. Koschenz. 2007. Application range of thermally activated building systems TABS. *Energy and Buildings* 39:593–8.
- Novoselac, A., and J. Srebric. 2002. A critical review on the performance and design of combined cooled ceiling and displacement ventilation systems. *Energy and Buildings* 34:497–509.

- R Development Core Team R. 2013. A Language and Environment for Statistical Computing. R version 2.15.3, Vienna, Austria.
- Rees, S.J., and P. Haves. 2001. A nodal model for displacement ventilation and chilled ceiling systems in office spaces. *Building and Environment* 36:753–62.
- Rim, D., and A. Novoselac. 2010. Ventilation effectiveness as an indicator of occupant exposure to particles from indoor sources. *Building and Environment* 45:1214–24.
- Sastry, G., and P. Rumsey. 2014. VAV vs. radiant. *ASHRAE Journal* 56:16–24.
- Schiavon, S., F. Bauman, B. Tully, and J. Rimmer. 2011. Ventilation effectiveness in combined chilled ceiling and displacement ventilation systems. *Proceedings of International Conference Indoor Air Quality and Climate, Austin, TX, June 5–10*.
- Schiavon, S., F. Bauman, B. Tully, and J. Rimmer. 2012. Room air stratification in combined chilled ceiling and displacement ventilation systems. *Science and Technology for the Built Environment* 18:147–59.
- Skistad, H., E. Mundt, P.V. Nielsen, K. Hagstrom, and J. Railo. 2002. *Guidebook n. 1, Displacement ventilation in non-industrial premises*. Brussels, Belgium: REHVA.
- Stetiu, C. 1999. Energy and peak power savings potential of radiant cooling systems in US commercial buildings. *Energy and Buildings* 30:127–38.
- Tan, H., T. Murata, K. Aoki, and T. Kurabuchi. 1998. Cooled ceiling/displacement ventilation hybrid air conditioning system—design criteria. *Proceedings of Roomvent, Stockholm, Sweden, June 4–17*. pp. 77–84.
- Thornton, B.A., W. Wang, M.D. Lane, M.I. Rosenberg, and B. Liu. 2009. *Technical support document: 50% energy savings design technology packages for medium office buildings*. Pacific Northwest National Laboratory, Richland, WA.
- Tian, Z., and J.A. Love. 2005. An integrated study of radiant slab cooling systems through experiment and building simulation. *Proceedings of 9th International IBPSA Conference, Montréal, Canada, August 15–18*, pp. 1229–36.
- Tian, Z., and J.A. Love. 2009. Energy performance optimization of radiant slab cooling using building simulation and field measurements. *Energy and Buildings* 41:320–30.